LASER METAL DEPOSITION OF FUNCTIONALLY GRADIENT MATERIALS FROM ELEMENTAL COPPER AND NICKEL POWDERS

S. Karnati*, T.E. Sparks*, F.Liou*, J.W. Newkirk†, K. M. B. Taminger‡, W. J. Seufzer‡

*Department of Mechanical Engineering, Missouri University of Science and Technology, Rolla MO, 65409
†Department of Materials Science and Engineering, Missouri University of Science and Technology, Rolla, MO, 65409
‡NASA Langley Research Center, Hampton, VA
REVIEWED

Abstract

This work deals with the planning and fabrication of a functionally gradient copper-nickel composition via Laser Metal Deposition (LMD). Various compositions of copper and nickel were made by blending different weight percentages which were then sequentially deposited to fabricate functionally gradient copper-nickel thin-wall structures. Analyses were performed by sectioning the thin-wall samples for metallographic, hardness, X-ray diffraction (XRD) and Energy Dispersive X-ray Spectroscopy (EDS) studies. The fabrication was studied for identifying and corroborating the deposited compositions and their corresponding gradients. XRD analyses were performed to identify the crystal structure of the deposit. EDS analysis was instrumental in identifying the variation in composition and realizing the gradient in between compositions. Consequences of using different laser beam intensity profiles and varying laser power duty cycles were realized by analyzing the copper-nickel concentration trends obtained from EDS analyses. Hardness testing was successful in capturing the decreasing trends in strength with decreasing nickel concentration.

Introduction

The concept of grading materials was first proposed by material scientists in Japan as a means for preparing thermal barrier materials [1]. Functionally Graded/Gradient Materials (FGM) are materials which gradually change in material composition or microstructure along a specific dimension. These materials can be tailored to serve specific purposes and the gradual change in properties leads to lower residual stresses and also increases durability [2]. In today's research the concept of FGM is being applied to serve various purposes in fields such as bio-medical, aerospace, automotive, electronics etc. [3, 4].

The list of potential techniques for manufacturing FGMs is extensive. For example, plasma spraying [5], die compaction [6-8], powder metallurgy [9], slip casting [10] and additive manufacturing [11-15] have all been employed to demonstrate the manufacture of FGM's. However additive manufacturing has advantages due to its potential for achieving premium material properties and fabricating complex geometries [20]. The layer by layer build schema and the use of powder to supply materials will enable the manufacture of complex geometries with controllable gradients [16].

A significant number of studies have been conducted on the output attributes achieved from fabricating FGMs via additive manufacturing techniques. The studies involved researching the variations in properties achieved through grading in, strength, toughness, hardness, corrosion

resistance, microstructure, and thermal resistance [11-18]. All of the above referenced work though was primarily limited to identifying the viability of manufacturing the graded material via laser metal deposition processes. The materials were chosen in order to introduce or better the properties of the FGM, properties that were characteristic to the constituent materials. These fabrications were constrained by the limited compatibility that existed between the materials. Also, in few cases the formation of intermetallic compounds proved detrimental to the fabrication of the FGM's [21]. Previously attempts have been made to improve the stiffness of a parent material by adding ceramic materials. Graded structures were deposited by varying the volume fraction of the ceramic material being added. However the limitation to this approach was the maximum amount of ceramic material that could be added. Beyond a certain volume percentage the structure lost its integrity and high degrees of porosity was observed [22]. Also, most of the chosen materials were pre-alloyed powders. While the number of studies conducted in this area are voluminous, it is the author's belief that our understanding of the process is still far from complete. This research will elaborate on not just the manufacturing of copper-nickel FGM's, but also the use of elemental materials to manufacture alloy composition FGM's and the role of the laser employed to manufacture the FGM.

This research chooses to functionally grade copper and nickel using LMD owing to the uniqueness of material characteristics that can be achieved. Copper is an excellent material for applications requiring improved thermal conductivity and resistance to oxidation in salt and alkaline atmospheres. Nickel is one of the major constituents of high temperature alloys which possess high strength and toughness at extreme temperature regimes. The higher temperature limit for oxidation is also an added benefit of using nickel. Combing the thermal conductivity of copper and high temperature strength of nickel could prove worthwhile for manufacturing high temperature viable components. The characteristic of complete solubility of copper in nickel and vice-versa was particularly beneficial in understanding the fabrication procedure for successfully manufacturing the copper-nickel FGM. Compositions blended in varying weight percentages of nickel and copper were deposited sequentially to fabricate the FGM. A diode laser and a fiber laser were employed to manufacture the FGM, the effects of different laser beam intensity profiles on the concentration gradients was successfully realized through EDS analyses. The effect of varying duty cycle was also successfully investigated.

Experimental procedure

A schematic diagram of the deposition process is shown in Fig. 1. The constituents of the system are the laser, powder feeder and CNC worktable.

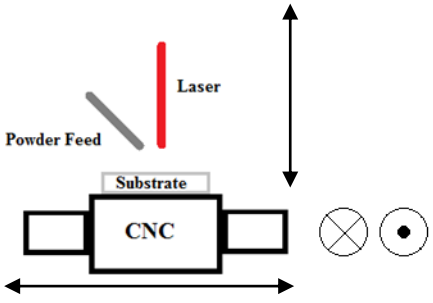

Figure 1. Schematic diagram of the setup for deposition process (arrows indicate the possible directions of motion)

The lasers used were a Nuvonyx diode laser with a maximum power of 1 kW, an operating wavelength of 10.64 micron and a top-hat beam intensity profile and an IPG photonics fiber laser with an operating wavelength of 1 micron and a Gaussian beam intensity profile. The substrate was placed at a distance of 250 mm in the laser's focal plane. A model 1200 Baystate Technologies powder feeder was used to deliver powder for deposition. The substrate was mounted on 5 axis FADAL CNC for deposition. The spot size of the laser was measured to be approximately 2 mm. The deposition was performed in an Argon atmosphere. The substrates chosen were Stainless Steel 304 (SS304) pieces whose dimensions were 30mm in length, 12mm in width and 6.5 mm in thickness.

Copper and nickel powders were acquired from Atlantic Engineering Equipment and were of 99.9% purity. The nickel powder was spherical gas atomized powder with a particle size distribution of -100 and +325 mesh. The copper powder though was irregular with a particle size distribution of -100 and +325 mesh. The powders were baked at 160^{o} C in a furnace to completely dehydrate the powder. The blends deposited and their deposition sequence is shown in Tab. 1 and Fig. 2 respectively.

Element	Blend 1	Blend 2	Blend 3	Blend 4
Cu (weight %)	0	25	50	75
Ni (weight %)	100	75	50	25

Table 1. Blends of elemental powder used for FGM fabrication

The powder blends were deposited on substrate in the order as shown in Fig. 2. Blend 1 was chosen for preliminary deposition since it has the highest melting point of all (100% Ni). The blend 4 was limited to 75% of Cu due the high reflectivity of the material wherein deposition of 100 % Cu is not feasible using the current lasers. Each blend was deposited up to a height of approximately 4 mm. A constant power of 700 W and a scan speed for 300 mm/min was used to carry out the depositions.

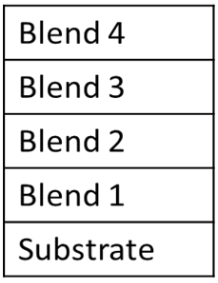

Figure 2. Schematic representation of deposited FGM

The deposited FGM was sectioned, mounted in Bakelite and polished for metallographic and EDS analyses. EDS analysis was performed on FEI Helios Nanolab 600 FIB/FESEM using an Oxford Energy Dispersive Spectrometer. The acceleration voltage and beam current for the EDS analysis were 20 kV and 1.4 nA.

Microstructure analysis was performed after etching the FGM for Ni. The etchant used was 100 ml of nitric acid and acetic acid mixed in a 1:9 volume ratio respectively. Vickers hardness testing at a 10 gm load was performed to study the variation in mechanical properties

RESULTS AND DISCUSSIONS

Copper and nickel are completely soluble in each other, which the authors theorized to ensure a hassle free deposition. Figure 3 shows the phase diagram of Cu and Ni which indicates a lack of intermetallics or line compounds for the chosen system of elements. The output at all compositions of copper and nickel is single phase solid solution. Hence the fabrication in a metallurgical perspective was theorized to be feasible.

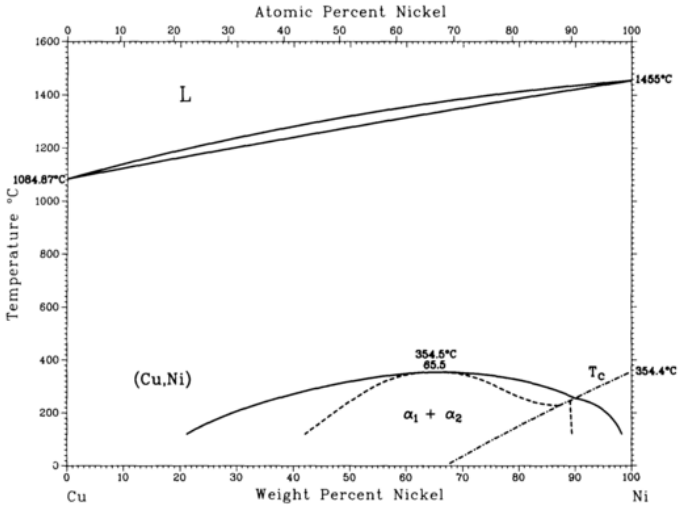

Figure 3. Cu-Ni binary phase diagram, it indicates no possible intermetallics and a single phase solid solution at all compositions of nickel and copper [19]

As expected, the deposit forms a single phase solid solution (as seen in figure 3). The same was confirmed from the X-Ray Diffraction (XRD) analysis. XRD plots were examined from different sections of the FGM (figure 4) and the analysis confirmed that the output was a single phase solid solution. It was also identified that, with increasing content of Cu the XRD pattern drifted from nickel's characteristic positions towards copper.

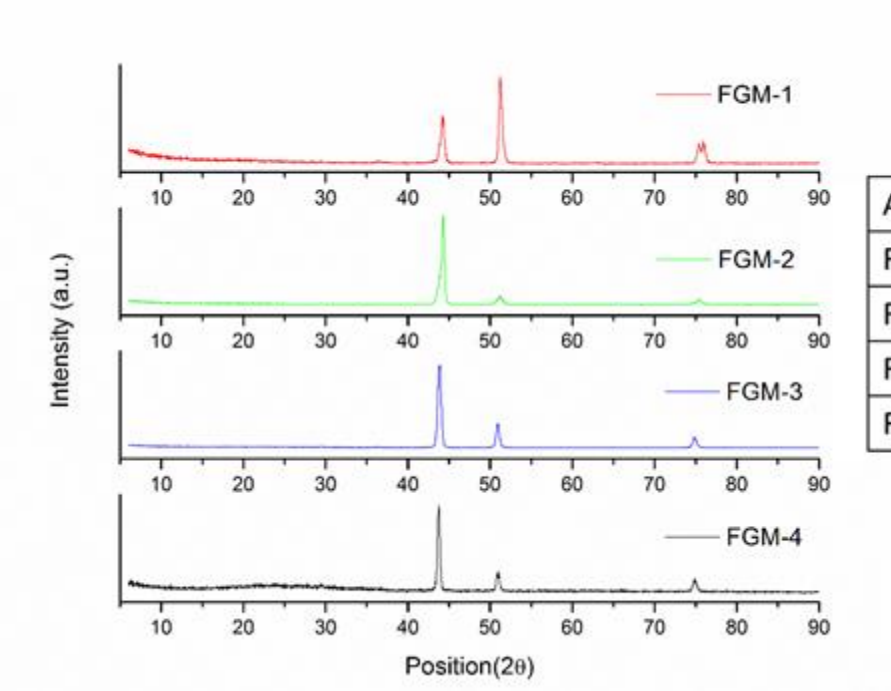

Approximate site of analysis	
FGM-1	75 % Ni
FGM-2	50% Ni
FGM-3	25% Ni
FGM-4	20% Ni

Figure 4. XRD patterns acquired along the height of the FGM indicating a single phase solid solution. A peak shift from nickel's characteristic pattern to copper's indicating increasing amount of copper was noticed

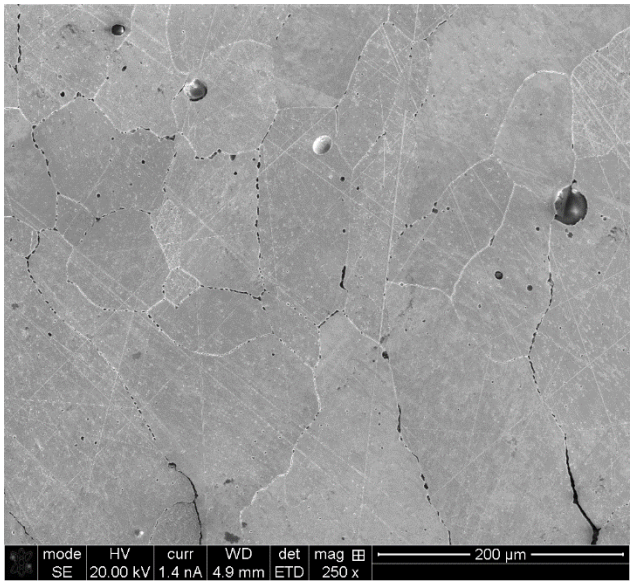

Figure 5. Microstructure of 100% wt. Ni, an equiaxed single phase microstructure with and average grain size of 138 micron

Figures 5 through 8 are the etched microstructures obtained from sections along the height of the deposit (fabricated using the top hat beam laser). Figure 8 shows the microstructure of the section of FGM that corresponds to 100 % Ni. It's a single phase equiaxed microstructure. The average grain size (by measuring the longest dimensions of the grains in the obtained

micrographs) is determined to be 138 micron. It can be noticed that gas porosity and inter-granular porosity has occurred in this section.

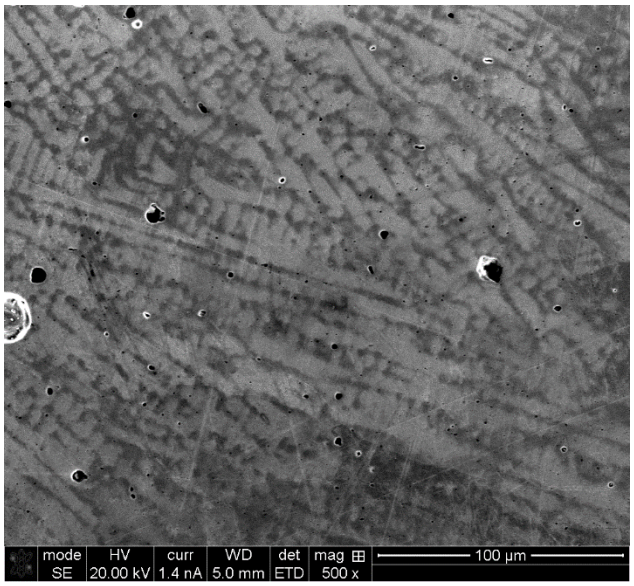

Figure 6. Single phase microstructure of 75% wt. Ni, with an average grain size of 179 micron

Figure 6 depicts the microstructure of the section of FGM that corresponds to 75% wt. Ni, 25% wt. Cu. From the image it can be seen that the rapid solidification has caused a variation in the amount of Nickel solidified in the deposit. The bright dendritic phase solidified first and hence has a higher concentration of nickel while the dark matrix is copper rich. The average grain size was measured to be 179 micron. Gas porosity was noticed in the deposit, same as in the case of 100 % wt. Ni.

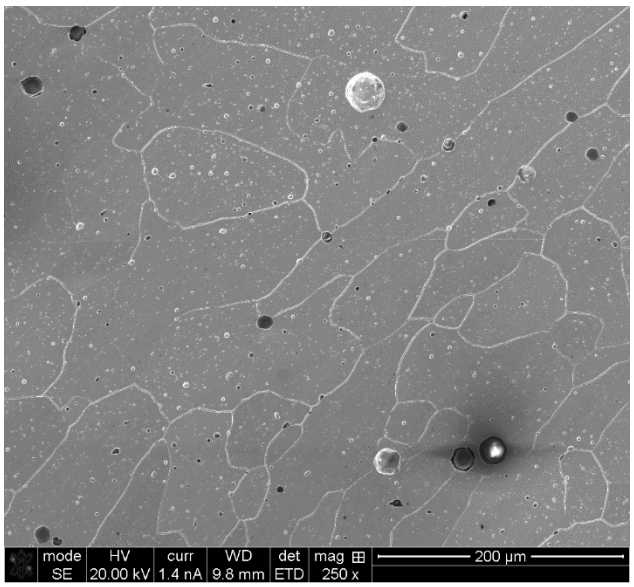

Figure 7. Single phase microstructure of 50% wt. Ni with an average grain size of 135 micron

Figure 7 shows the microstructure of the section of the FGM that corresponds to 50% wt. Ni, 50% wt. Cu. The microstructure indicates an equiaxed single phase microstructure. The average grain size was calculated to be 135 micron. Gas porosity was noticed even this is section.

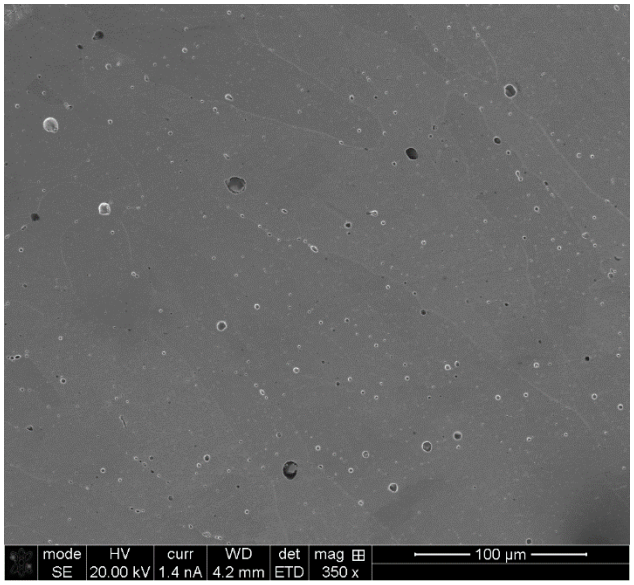

Figure 8. Single phase microstructure of 25% wt. Ni with an average grain size of 151 microns

Figure 8 shows the microstructure of 25% wt. Ni in the FGM. A single phase microstructure comprising columnar and equiaxed grains was noticed. The calculated average grain size was noticed to be 151 microns. Similar gas porosity was noticed in this section too.

The nickel rich sections of the deposit contained a significant amount of porosity. A series of experiments were carried out identify parameters that could yield low porosities, it was then concluded that the source of porosity was not solvable through process parameter modifications. The spherical shape of the porosity indicated that it was a consequence of gas evolution during solidification. The source of the gas was expected to be nickel oxide. It was theorized that the lower thermal stability of the oxide results in dissociation and oxygen gas evolution. The higher viscosity and surface tension of molten nickel was also expected to support the survival of porosity during solidification [23]. The data in table 2 specifies the temperature dependent surface tension values of molten Ni and Fe for comparison, the values imply a higher probability for pore survival in molten nickel.

Element	Surface tension (dyne/cm)	Temperature range
Ni	0.215t+ 1665	t ϵ [1475C, 1650 C]
Fe	0.65t+773	t ϵ [1550C, 1780 C]

Table 2. Temperature dependent surface tensions of molten Ni and Fe

Acknowledging high degrees of porosity formation, investigation was further carried on for composition studies. EDS analysis was performed through the height of the FGM to identify and validate the composition variations in the deposit. The interfaces between sections of the FGM were identified and the variation in concentrations of Cu and Ni was realized by comparing the Ka 1 intensity in the EDS analysis. The effect of different laser beam intensity profiles was analyzed by identifying interface and measuring the distance from the interface to the start of the

saturated region. Figure 9-12 indicate EDS line scan data acquired across the interfaces 100-75, 75-50 and 50-25 % Ni. Figure 9 and 10 indicate the line scan data gathered from the 100-75 and 75-50 interfaces on the FGM manufactured using the Gaussian beam laser. The saturation between blends was seen to occur in a single and sudden rise/drop in copper/nickel respectively. The transition region was noticed to be approximately 80 micron in length. The cause for spikes/dips (see figure 9 and 10) in saturated regions was identified to be porosity.

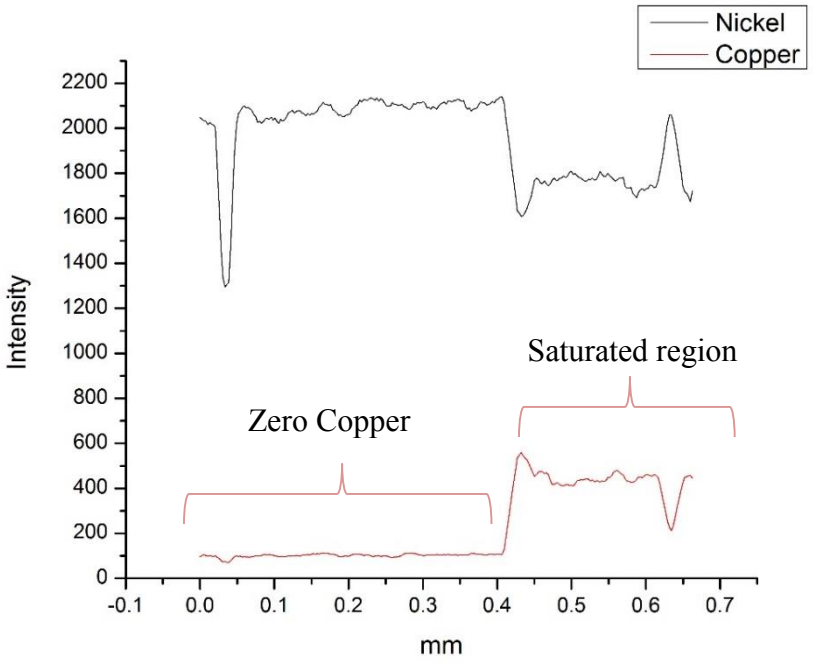

Figure 9. EDS line scan indicating the transition and saturation of Ni and Cu across the 100% - 75% wt. Ni interface (FGM made by Gaussian beam laser)

Figure 11 and 12 show the EDS line scans of the transition across the 75% to 50% wt. and 50% to 25% wt. Ni interfaces on the FGM manufactured employing the diode laser (top hat laser beam intensity profile). The transition was relatively much more gradual in this case in comparison to the previous fabrications (Gaussian beam intensity profile). The transition zone shown in figure 11, spanned approximately for 2 mm and the grading occurred in an almost linear fashion. After the transition the Ni wt. % stabilized at approximately 49 % wt. (measured by EDS point scan analysis, dwell time 10 min).

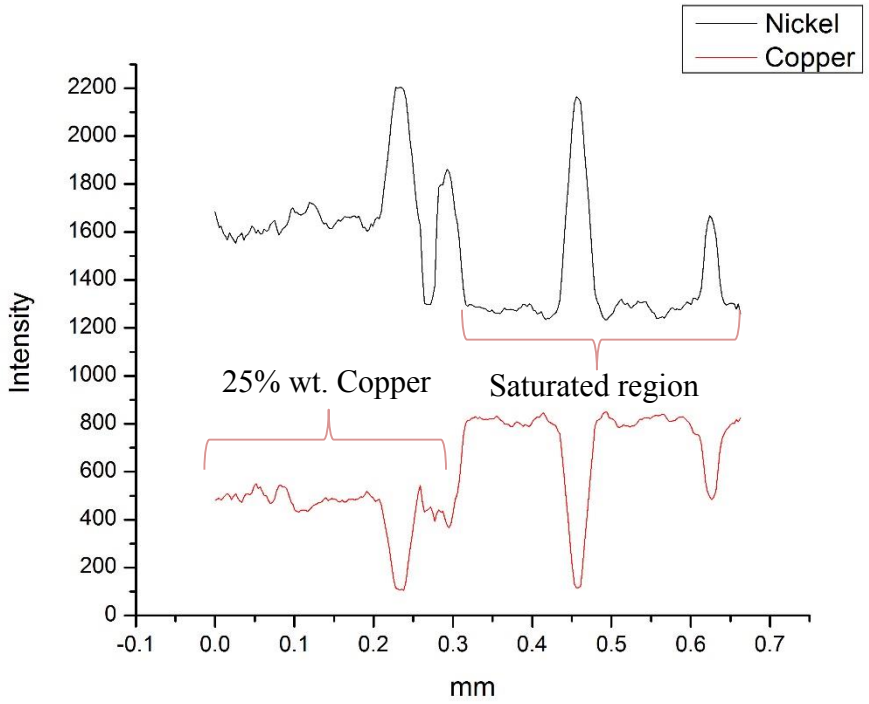

Figure 10. EDS Line scan analysis scan indicating the transition and saturation of Ni and Cu across 75%-50% wt. Ni interface in the FGM. The spikes in saturated regions were identified to be caused by porosity (FGM made by Gaussian beam laser)

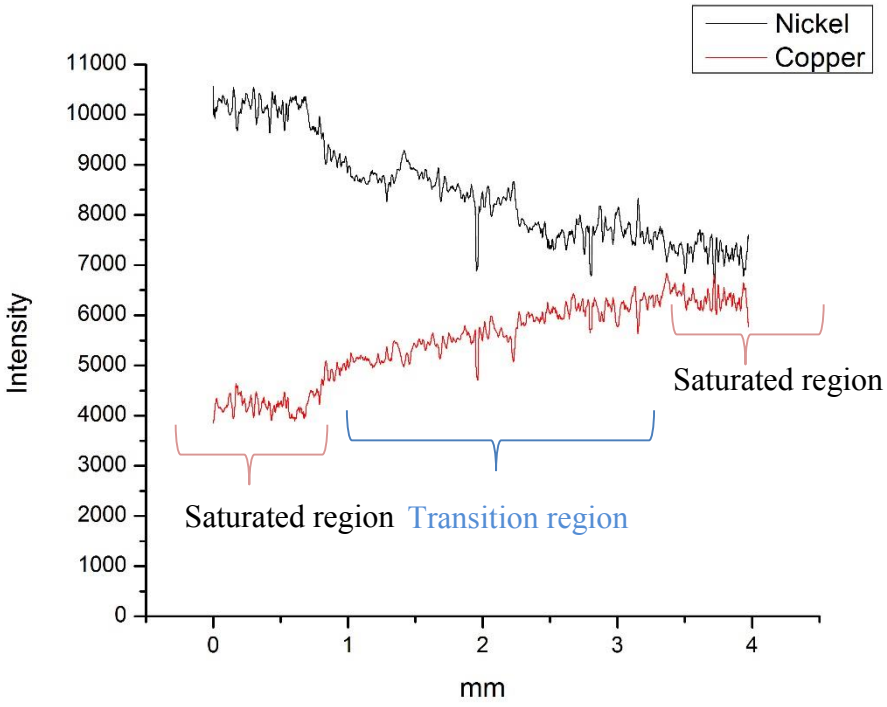

Figure 11. EDS line scan analysis of 75% -50% wt. Ni interface (made via top hat beam laser), indicating a transition length pf approx. 2mm

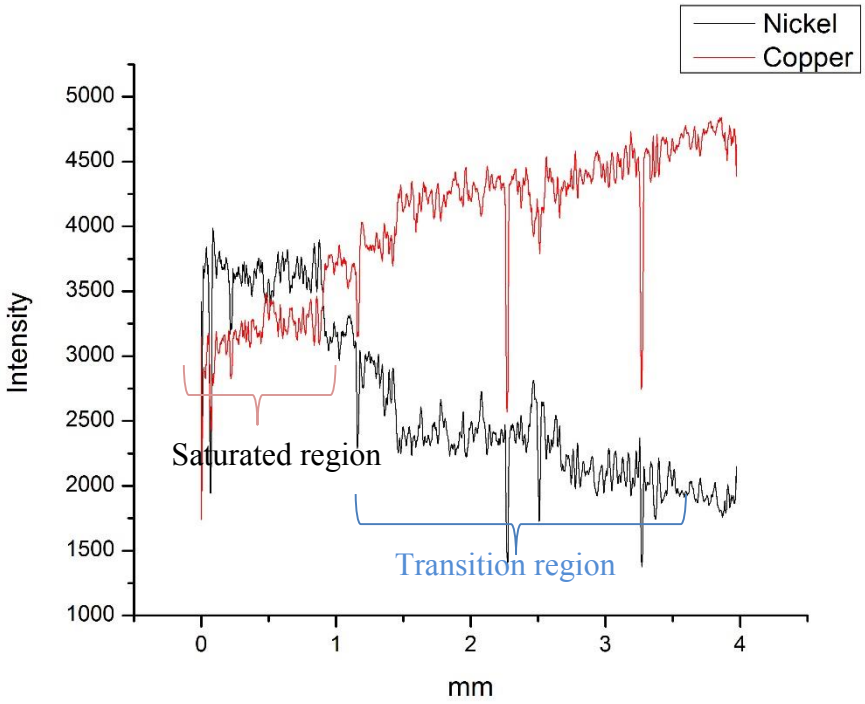

Figure 12. EDS line scan analysis of 50% -25% wt. Ni interface (made via top hat beam laser), indicating a transition length pf approx. 2mm. The dips/rises were caused by the porosity

Figure 12 shows the variation in nickel and copper EDS signal across the 50-25% wt. Ni interface (deposit manufactured using top hat laser). Point scan EDS analysis revealed that Ni was at 49% in weight before the transition. Post transition the Ni weight % stabilized at 25%. Figure 12 indicates the EDS line scan analysis of the same interface. It was again found that the main constituents of the deposit were Cu and Ni. The weight % of Cu was seen to rise from 50% to 75%. The interface spanned approximately for 3 mm. The cause for dips/rise in signal was identified as porosity.

Laser beam intensity profile has been identified to be a significant factor in tailoring the transition between blends during FGM fabrication. The difference in transition length is theorized to be a consequence of different remelting depths. At same amount of power and spot size the peak intensity for a Gaussian beam profile laser will be higher than the peak in top hat beam profile laser. The top hat beam laser would produce a shallower melt pool and thereby would result in lower remelting and thus result a lower dilution. Whereas in a Gaussian beam laser the remelting depth is more and therefore the transition would be large and the transition length would be small [25]. Hence, a Gaussian beam was concluded to produce a transition with tighter control. It was theorized that at a constant power and spot size, varying the duty cycle would produce different remelting depths and a tailored FGM could be fabricated with a relatively smaller transition length. Powder blend of 50 % wt. nickel and 50% wt. copper was deposited on a nickel substrate (fabricated via deposition) using the Gaussian beam laser. Duty cycle (constant power of 500W and scan speed of 300 mm/min) was varied from 100 % to 75% and 50% during three consecutive layers of deposition to create layers with different compositions. Figure 13 indicates the EDS line scan analysis across transverse sections of the three layer deposit. The three layers can be distinctly identified by the different compositions.

The transition between layers can be easily identified and the transition length is minimum when compared to the top hat top hat beam fabrication.

To identify the variation in the mechanical properties, a Vickers hardness analysis was performed across the length of the deposit. A 10 gm load was used to perform the indentation and evaluate the hardness values. Figure 14 is a plot of the variation in hardness obtained by plotting hardness values acquired at 0.5 mm spacing along the height (dimension of grading) of the FGM. The origin corresponds to the substrate (SS 304) of the deposit and the end of the plot corresponds to the 25% wt. Ni section of the deposit. As expected the hardness values of the deposit were observed to decrease, which further confirms the decreasing content of Ni across the deposit. The rise in hardness in the initial section was attributed to the increasing amount of Ni (substrate was SS 304) and the later drop was expected to be associated with the decreasing amount of nickel.

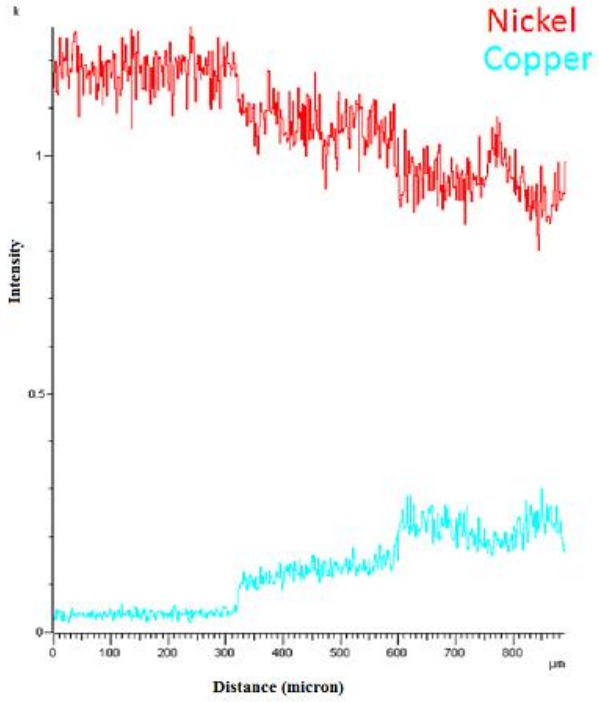

Figure 13. EDS line scan across the three layers deposited with varying duty cycle, indicates 2 different compositions occurred with a span of approx. 300 micron each

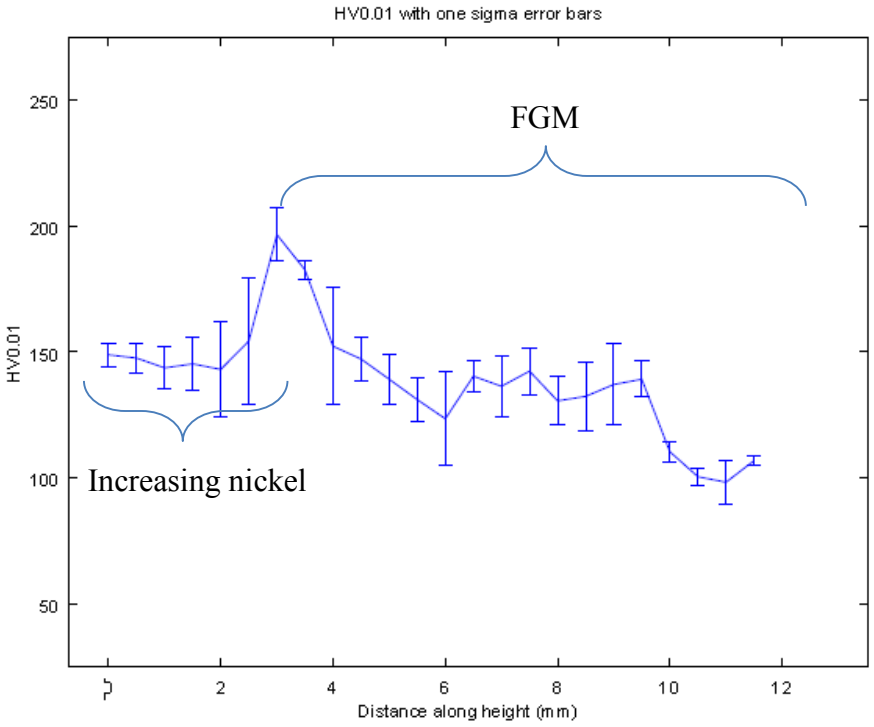

Figure 14. Hardness values indicating a decreasing trend across the height of the FGM (Gaussian beam)

CONCLUSIONS

A successful fabrication of a FGM of Cu-Ni composition was carried out. Mixtures of elemental Cu and Ni were blended and the blended mixtures were successfully laser deposited. A sectioned sample of the FGM was analyzed to corroborate the occurrence of the grading. Metallographic and EDS analyses were instrumental in identifying the phase and concentration details of the deposit. EDS analysis was crucial in identifying the concentration variation in the deposit. Interfaces between the sections of blends were identified and the approximate span of each transition was measured. The effects of laser beam intensity profile were successfully studied and it was concluded that Gaussian beam profile produced a smaller transition length. The idea of varying duty cycle to tailor transition was also successfully studied and EDS analysis concluded that distinct compositions were deposited. The variation in mechanical properties was identified by measuring the Vickers hardness values. Despite a few porosity issues the deposit was considered to be successful.

Acknowledgments

The authors would like to express their sincere gratitude to the support from National Aeronautics and Space Administration EPSCoR program (Grant# NNX13AM99A), and Intelligent Systems Center at Missouri University of Science and Technology.

References

[1] KOIZUMI, M., 1997, "FGM ACTIVITIES IN JAPAN", Compos Part B: Eng, 28 (1997), pp. 1–4

[2] W. Liu, J.N. DuPont, "Fabrication of functionally graded TiC/Ti composites by laser engineered net shaping", Scripta Mater, 48 (2003), p. 1337

[3] G. Sun, G. Li, S. Hou, S. Zhou, W. Li, Q. Li "Crashworthiness design for functionally graded foam-filled thin-walled structures", Mater Sci Eng A, 527 (2010), pp. 1911–1919

[4] A. Bandyopadhyay, B. Krishna, W. Xue, S. Bose, "Application of Laser Engineered Net Shaping (LENS) to manufacture porous and functionally graded structures for load bearing implants", J Mater Sci: Mater Med, 20 (2009), pp. 29–34

[5] Y. Miaymoto, W.A. Kaysser, B.H. Rabin, A. Kawasaki, R.G. Ford, "Functionally graded materials: design, processing, and applications", Kluwer Academic Publishers (1999)

[6] U. Leushake, A.N. Winter, B.H. Rabin, B.A. Corff, "General aspects of FGM fabrication by powder stacking", Mater Sci Forum, 308–311 (1999), pp. 13–18

[7] R. Watanabe, A. Kawasaki, M. Tanaka, J.-F. Li, "Fabrication of SiC–AlN/Mo functionally gradient material for high temperature use", Int J Refract Met Hard Mater, 12 (1993), pp. 187–193

[8] W.W.A. Gooch, "Development and ballistic testing of a functionally gradient ceramic/metal applique", Mater Sci Forum, 308 (1999), pp. 614–621

[9] Thummler F, Oberacker R. "An introduction to powder metallurgy", Institute of materials. London; 1993. p. 177–80.

[10] B.R. Marple, J. Boulanger, "Graded casting of materials with continuous gradients", J Am Ceram Soc, 77 (1994), pp. 2747–2750

[11] Tomasz Durejko, Michał Ziętala, Wojciech Polkowski, Tomasz Czujko, "Thin wall tubes with Fe3Al/SS316L graded structure obtained by using laser engineered net shaping technology", Materials & Design, Volume 63, November 2014, Pages 766-774

[12] Ting-ting QIAN, Dong LIU, Xiang-jun TIAN, Chang-meng LIU, Hua-ming WANG, "Microstructure of TA2/TA15 graded structural material by laser additive manufacturing process", Transactions of Nonferrous Metals Society of China, Volume 24, Issue 9, September 2014, Pages 2729-2736

[13] H.S. Ren, D. Liu, H.B. Tang, X.J. Tian, Y.Y. Zhu, H.M. Wang, "Microstructure and mechanical properties of a graded structural material", Materials Science and Engineering: A, Volume 611, 12 August 2014, Pages 362-369

[14] Kamran Shah, Izhar ul Haq, Ashfaq Khan, Shaukat Ali Shah, Mushtaq Khan, Andrew J Pinkerton, "Parametric study of development of Inconel-steel functionally graded materials by laser direct metal deposition", Materials & Design, Volume 54, February 2014, Pages 531-538

[15] Waheed Ul Haq Syed, Andrew J. Pinkerton, Zhu Liu, Lin Li, "Coincident wire and powder deposition by laser to form compositionally graded material", Surface and Coatings Technology, Volume 201, Issues 16–17, 21 May 2007, Pages 7083-7091

[16] Santos E C, Shiomi M, Osakada K, Laoui T, "Rapid manufacturing of metal components by laser forming", International Journal of Machine Tools & Manufacture, 2006, 46: 1459−1468

[17] R. Banerjee , D. Bhattacharyya, P.C. Collins, G.B. Viswanathan, H.L. Fraser, "Precipitation of grain boundary a in a laser deposited compositionally graded Ti–8Al–xV alloy – an orientation microscopy study", Acta Materialia 52 (2004) 377–385

[18] Ting-Ting Qian, Dong Liu, Xiang-Jun Tian, Chang-Meng Liu, Hua-Ming Wang, “Microstructure of TA2/TA15 graded structural material by laser additive manufacturing process”, Trans. Nonferrous Met. Soc. China 24(2014) 2729−2736
[19] “Cu (Copper) Binary Alloy Phase Diagrams”, Alloy Phase Diagrams, Vol 3, ASM Handbook, ASM International, 1992, p 2.167–2.182
[20] Muller, P., Hascoet, J.-Y., Mognol, P., “Toolpaths for additive manufacturing of functionally graded materials (FGM) parts”, (2014) Rapid Prototyping Journal, 20 (6), pp. 511-522.
[21] Tomasz Durejko, Michał Ziętala, Wojciech Polkowski, Tomasz Czujko, “Thin wall tubes with Fe3Al/SS316L graded structure obtained by using laser engineered net shaping technology”, Materials & Design, Volume 63, November 2014, Pages 766-774
[22] Yongzhong Zhang, Zengmin Wei, Likai Shi, Mingzhe Xi, “Characterization of laser powder deposited Ti–TiC composites and functional gradient materials”, Journal of Materials Processing Technology, Volume 206, Issues 1–3, 12 September 2008, Pages 438-444
[23] Ellingham diagram, F.D. Richardson JISI (1948)
[24] M. E. Fraser, w-k. Lu, a. E. Hamielec, and r. Murarka, “Surface Tension Measurements on Pure Liquid Iron and Nickel by an Oscillating Drop Technique”, Metallurgical Transactions, Volume 2, March 1971-817
[25] W. Steen, J. Mazumder, K. G. Watkins “Laser material processing”, Springer publications